Framework for extracting rails and setting-out railway line axis based on

UAV photogrammetric measurements

Pawel Burdziakowski [a)*], Cezary Specht [b)], Andrzej Stateczny [a)], Mariusz Specht [c)], Pawel S. Dabrowski [b)], Oktawia Lewicka [b)]

[a)] *Department of Geodesy, Faculty of Civil and Environmental Engineering, Gdansk University of Technology, Narutowicza 11-12, 80-233 Gdansk, Poland; pawel.burdziakowski@pg.edu.pl (P.B.), andrzej.stateczny@pg.edu.pl (A.S)*

[b)] *Department of Geodesy and Oceanography, Gdynia Maritime University, 81-347 Gdynia, Poland; c.specht@wn.umg.edu.pl (C.S.); p.dabrowski@wn.umg.edu.pl (P.S.D.); o.lewicka@wn.umg.edu.pl (O.L.)*

[c)] *Department of Transport and Logistics, Gdynia Maritime University, 81-225 Gdynia, Poland; m.specht@wn.umg.edu.pl (M.S.)*

*) correspondence author

Abstract: Technical diagnostics enables assessing the current technical condition of a railway line and adjacent infrastructure, and to forecast its changes over a specific time horizon. One of its elements is the periodic monitoring of rail position and their geometry. The article presents a new framework for the setting-out of a railway track axis. The process presented in the manuscript is based on the specific filtration and extraction of rails from a point cloud originating from the photogrammetric process. Data was acquired using a small unmanned aerial vehicle (UAV). A railway track axis setting-out using the process described herein was related to dynamic satellite track measurement. An average accuracy achieved in the horizontal plane is 1.6 cm which corresponds to the accuracy of the source photogrammetric product. The achieved accuracy enables using this method to be suitable for technical track monitoring, geoinformation and cartographic work.

Keywords: UAV, railway line, photogrammetry, extraction, point cloud

1. Introduction

Rail transport plays a significant role in everyday life. Railway lines transport millions of people

and tons of goods, which from a social and economic perspective, is a crucial element of each nation's economy. As a result, maintaining an adequate technical condition of railway infrastructure will ensure the required smooth flow of goods, transport security, minimized maintenance costs and limited losses due to failures [1].

An integral part of the railway infrastructure maintenance process is technical diagnostics. It enables evaluating the current technical state and predict its changes over a specific time horizon. Various measurement techniques are used to this end - starting with classic surveying, through satellite techniques, to spatial measurements utilizing photogrammetry and laser scanning. Spatial measurement products, such as point clouds (PC), digital surface models (DSM) and orthophotomaps enable visualizing and developing a detailed railway line model (together with adjacent infrastructure), as well as monitoring geometric changes within the studied infrastructure, detecting collision elements, locating deformations and damage, constructing a full database of objects within a given railway line. Predicting the technical condition of the railroad based on spatial measurements can also be achieved.

Mobile laser scanning (MLS) and airborne laser scanning (ALS) enable the fastest and most accurate creation of a spatial model for large objects [2,3]. Therefore, they have been successfully applied for monitoring and stock-taking of railway infrastructure for many years. Classic example of mobile laser scanning involves a laser scanner installed on-board a rail vehicle that moves along a specified route. The collected spatial information is then subject to processing using numerical methods, leading to the extraction of relevant data. An interesting example of such a technique has been presented by Elbernik et al. [4]. The authors described a method for the automatic extraction of railway line axes based on mobile laser scanning, which enabled achieving an accuracy of 2-3 cm. In another paper [5], Lou et al. demonstrated a quick algorithm for the automatic extraction of railway track in real-time, using data from a small Velodyne VLP-16 Lidar. It should be emphasized that the VLP-16 Lidar is very popular also in the case of other real-time mobile applications [6] and enables achieving a measurement accuracy below 2 cm. In yet another publication [7], the researchers presented a method for the extraction and modelling of a railway track course and related overhead contact line based on a system of two integrated lidars. In this case, the mobile system generated a point cloud with a density of as many as 700 points per square meter (pts/m2). The authors of [8] introduced a complete procedure involving the use of ALS and MLS data for the reconstruction and modelling of a railway line with trackside infrastructure and other adjacent objects. Here, the researchers used a mobile system based on two Riegl scanners, which enabled achieving a data density equal to 720 pts/m2. Mobile laser scanning was also applied as part of [9], which

presented a precise algorithm for extracting railway tracks, based on a point cloud. An undoubted advantage of modern laser systems is the high density of the resulting point cloud, which allows to precisely map the structural geometry.

Methods for extracting relevant data based on laser scanning are also supported by image data. An image is used to eliminate redundant data, as well as to obtain qualitative data or supplement spatial information about an object. In their work, Soni et al. [10] demonstrated a comprehensive method involving the application of close-range photogrammetry and laser scanning to monitor railway infrastructure. In another publication [11], Beger et al. presented a very interesting method combining image data from aerial photos with airborne laser scanning. Because scanner data exhibits a slightly lower density (from 60 to 90 pts/m2), this was integrated with an orthoimage with a ground sampling distance (GSD) of 5 cm/pix. The orthoimage was used to develop a mask, which enabled eliminating ALS points not belonging to the railroad. Such a procedure, when implemented to deal with the large amount of data for a long railway line section, significantly accelerated and improved the quality of the research. Within the practice, the track axis extraction itself is based only on data derived from laser scanning. In [12], the researchers also demonstrated a similar technical solution, based on data derived from an airborne laser scanner and a high-resolution camera. Therein, devices installed on-board a helicopter enabled achieving a point cloud density and GSD similar to the values in the work by Beger et al.[13] Kaleli et al. [13] presented an algorithm for extracting a railway line based on an image obtained from a single camera at the head of a rail vehicle. While the algorithm extracts railway line data, the method does not allow for setting-out the geographic position of the studied track course. A similar solution was suggested in [14], which used image data more extensively. Image is also a very good source of information on the condition of the rail head and adjacent infrastructure [15–18] or even other selected rail vehicle elements [19–21].

The issue of visual rail track surface inspection, technical diagnostics or acquisition of spatial information is also made possible using unmanned aerial vehicles (UAV). A common feature associated with employing UAVs for inspecting or studying railway track routes is that they do not require suspending traffic within the studied route. Furthermore, using UAV is very safe for people, since they do not have to work near the track. An undoubted advantage of acquiring data via unmanned aerial vehicles is their relatively low cost and the possibility of quick deployment at the take-off site. The flight and measurements themselves can be implemented at a low altitude, still ensuring the safety of such an operation. The data acquired from UAV are as accurate as that obtained from manned aircraft, and as some studies show,

even more accurate owing to the development of this technology [22]. Interestingly, UAV can fly over a specific railway line guided by the image itself [23,24]. Such an approach enables precise flight trajectory control, without the need for having the geographic positions of the studied railway line in advance, in order to program the flight route.

A relatively simple approach was presented by Singh et al. in [1]. based on an image[1]. The algorithm presented there is based on image conversion from RGB to HSV, and the converted image is subjected to contextual and morphological filtering. Other operations on a digital image from a UAV, intended for extraction of relevant trackage features were discussed by Branic et al. in [25]. In this case, UAV-sourced images were analysed with methods primarily used to extract features, similar to cameras fitted on vehicle heads. Sahebdivani et al. [26], also employed a commercial UAV, however, in the case of their work, railway tracks were identified and localized based on a point cloud created during photogrammetric processing. Other very extensive research work [22] demonstrated a precise photogrammetric system based on a high-resolution camera mounted on-board a UAV, and intended for inspecting port crane rails. An unprecedented GSD of 0.9 mm was achieved within this study. As proven, using UAV photogrammetry enables precisely inspecting the trackage and developing a model with an XY plane accuracy up to 3 mm. As shown in [27], images acquired from a UAV are a very good source of data for studying the railhead surface.

UAVs are capable of carrying not only cameras, but also laser scanners. As evidenced by Geng et al. in [28], such a solution is effective for the purposes of inspecting railway infrastructure. This technology enables constructing a railway line model with a horizontal plane accuracy of 6 cm, and a vertical plane accuracy of 7 cm [29].

A common characteristic of railway track extraction methods from point clouds and using laser scanning is a procedure based on geometric features. Laser scanning point clouds are very accurate, and are true to actual geometry. Even minor differences in height are mapped on the scan, which enables using the various geometric properties of a studied cloud for extraction, and consequently, precisely extracting a railhead data. Moreover, a laser scanner point cloud is very sharp, which means that edges are clear and all differences in the height are very accurately mapped. The same cannot be said about a cloud originating from a photogrammetric process. The edges therein are mapped less precisely and are smoother, while height differences are not so sharp and clear. Such a situation means that extraction methods used in the case of laser scanner clouds cannot be applied for extracting a rail track from a photogrammetric process cloud. Among other things, this fact motivated the development of a

method for extracting a railroad line from the point cloud created by the photogrammetric process.

Photogrammetric images hold information regarding the spectral response of an object, most usually expressed as an RGB (Red, Green, Blue) colour space model, which is a certain non-geometric (qualitative) feature. In such a case, data can be extracted from an image by employing contextual or non-contextual filters, morphology or computer vision methods. Because a point cloud originating from a photogrammetric process holds information on the colour of each point, it can be argued that tracks from such a cloud can be extracted using methods based on specific geometric and non-geometric methods (colour). This fact is precisely the basis for the solution. Using filtration based on the position of cloud points and their geometric relation (like for solutions based on laser scanner data), as well as the recorded spectral response of a point (colour) (like for the typical solution based on the images) and its relation with the immediate surroundings, the rails can be extracted.

This article presents a new method for the filtration and extraction of rails from a point cloud originating from a photogrammetric process. It is based on a two-stage extraction process. The process is based on the geometric features and spectral response of points. It thoroughly reviews the suggested solution and the applied data extraction algorithm. The designed algorithm has been presented based on actual data acquired during an extensive measurement campaign. The results obtained by proposed method have been compared to reference data obtained form satellite measurements. The paper lists the results associated with the accuracy of setting-out rail axes based on the method described herein.

This paper presents the following new solutions in the field of low-ceiling photogrammetry:

- a two-stage method for rail extraction and railway track axis setting-out from a point cloud acquired through a photogrammetric process using a UAV, based on geometric and non-geometric features of the cloud;
- validation of track axis setting-out results through comparing them with data acquired from precise measurements of the track axis using satellite methods.

The article consists of 4 sections. The first provides a review of the source literature and outlines the motivation behind solving the problem. The second (Materials and Methods) reveals information on the procedure, as well as a description of the proposed method. The Results section provides a demonstration of the applied measurement technology and a description of the conducted field tests, as well as a validation of the results. The article

culminates with conclusions, including an assessment of the developed procedure, applied technology and the developed extraction method.

2. Materials and Methods

2.1. Procedure

Figure 1 shows the applied research process and the data processing procedure. The entire data development process is commenced by a data acquisition block, which includes such typical activities as flight planning, photogrammetric matrix point (ground control points) measurements, photogrammetric camera calibration, etc.

The next block describes the data processing process. Image data acquired during a UAV flight was processed using typical photogrammetric software. In this case, the Agisoft Metashape (Agisoft LLC, Russia) software was used. The results included the usual products, such as a point cloud, digital surface model (DSM) and an orthophotomap, which are then mined to extract rails and to set out railway track axis position in the next step.

The basis for the extraction of rails is a dense point cloud, which is subjected to successive operations of initial filtration and rail extraction blocks. Detailed operations within these blocks are described later in this paper. Data processing leads to setting-out the railway line axis course. The developed method of extraction from the point cloud is based on geometric and non-geometric features of a point cloud originating from a photogrammetric process.

The proceeding sections of this paper discuss the used tools and methods, and presents details of the measurement data processing.
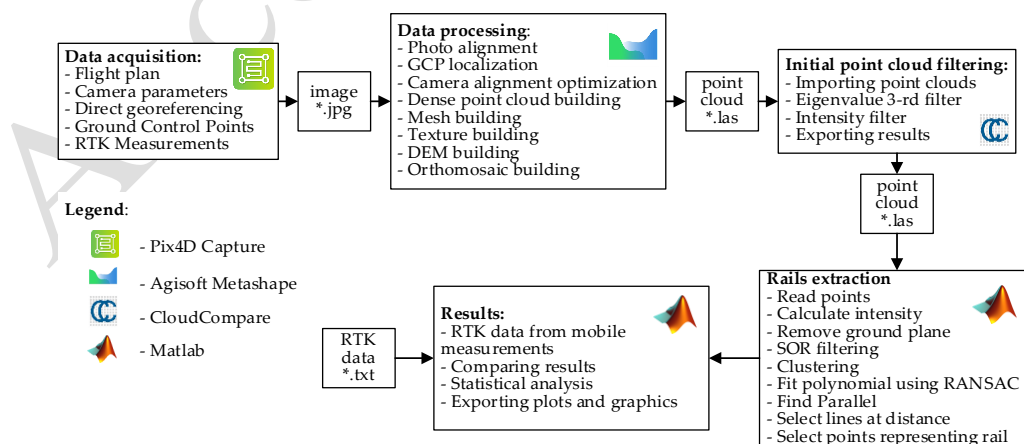

Figure 1. Research process

2.2. Initial point cloud filtering

In this work, a dense point cloud (1850 pts/m^2) upon which photogrammetric software was applied, was used to extract rails. Such a point cloud holds information on the spectral response of represented objects, expressed in R - red, G - green and B - blue components. In other words, the cloud contains information on electromagnetic radiation intensity of each of the spectral channels (I_R, I_G, I_B). In order to simplify further consideration, the authors converted spectral responses recorded separately in each channel to point intensity (I_p), according to the formula [30] :

$$I_p = 10(0.21 I_R + 0.72 I_G + 0.07 I_B) \tag{1}$$

Initial point cloud filtration includes three steps and is an integral part of the method presented herein. The first step is the manual and coarse railway line extraction. In this stage, the operator uses any appropriate software to mark the area that the railway line crosses. This is aimed at coarsely eliminating irrelevant data recorded by the UAV from the area.

The second initial filtration stage is based on principal component analysis (PCA), similar to [26,31–33]. Because a rail subgrade is usually designed and executed in a way so as to exhibit the least local elevation changes in the longitudinal track direction, the smallest third eigenvalue (λ_3) in the local vicinity of the studied point will be close to zero. In a situation where a group of cloud points will represent a rail or any other object, this value will be increasing. Therefore, all points that satisfies the condition:

$$\lambda_3 < 0.001, \tag{2}$$

are marked as belonging to a railway line. The value in the equation (2) was obtained based on the research [26,31–33], should be close to zero and in the presented research has been experimentally confirmed.

The rail itself usually has a different colour and is particularly contrasted against the bright aggregate, and such information may constitute the basis for extraction. Therefore, similar to the studies in [34] where rails were extracted using information on colours (RGB), we propose a novel approach, a colour extraction from a point cloud. In consequence, the first initial filtration step involves extracting points based on its intensity (I_p) calculated according to the equation (1). The filtration based on intensity, where:

$$I_p < 200 \tag{3}$$

leads to obtaining a point cloud that represents the rails and elements in the vicinity of these rails that exhibit similar intensity I_p to the rail itself. This value can be experimentally adjusted to match the mean intensity that is captured for the railroad rails.

2.3. Rail extraction

Rail extraction from a pre-filtered point cloud is based on multi-stage segmentation and classification. This stage is used to determine which point from a point cloud represents a rail, and which does not.

It commences with geometric filtration, which is the elimination of points not belonging to the ground, through fitting a plane model to a point cloud, and eliminating the points located at a distance greater than the adopted threshold (outliers). The M-estimator Sample Consensus (MSAC) algorithm is used to find a plane [35]. The MSAC algorithm is a variant of the RANdom SAmple Consensus (RANSAC) [36]. Therefore, further calculations take into account only the points located from the fitted plane model at a distance lower than D_i. The authors of this study assumed that the distance D_i was 1 meter, which can be expressed as follows:

$$D_i < 1 \tag{4}$$

The next step involved cleaning the cloud of individual point clusters that are commonly deemed as 'noise' and do not represent regular railway infrastructure shapes. These points usually depict small vegetation and slender elements of auxiliary railway infrastructure (poles, contact lines, posts), the geometry of which was not fully reconstructed in the photogrammetric process. For this purpose, the authors conducted filtration using the method in [37] , assuming that it eliminates individual points or clusters satisfying condition (5) for $n_{points} = 10$:

$$t_{in} < 1, \tag{5}$$

This means that the cloud is stripped of points located further than the threshold t_{in}. This threshold implies a single standard deviation from the mean value - all mean distances of neighbours for n_{points} from the studied point. Therefore, the point is considered an outlier if the mean distance to its n-closest neighbours is greater than the threshold t_{in}. The aforementioned operation result in a scrubbed point cloud depicting the rails and a small number of infrastructural elements directly adjacent to the rails. In consequence, successive stages involve eliminating these unwanted points and indicating only those representing the rails. To this end, subsequent operations involved dividing the cloud into clusters, fitting a polynomial to each cluster and marking only those points that fell within a pre-set threshold for the distance from the fitted polynomial.

The division of the cloud into clusters involves point cloud segmentation based on the Euclidean distance. In this case, the points belong to the same cluster if their mutual distance does not exceed a specified Euclidean distance D_e. It the studied cases, the value that was

adopted is that $D_e = 200$, therefore if the distance between the examined points is greater than D_e, it will belong to a different cluster. This enables dividing a cloud into homogeneous point clusters, which further facilitates calculations [38].

Another step involves finding a and b coefficients for the P polynomial (Equation 6) for each point cluster. This is achieved through sampling this set of points and generating polynomial matches of the line mode. As a result, the match with the most inliers within a distance of D_p is returned. Because a rail should be straight for a certain data cluster, the fitted polynomial (6) should estimate a given rail section as faithfully as possible. As previously, the M-estimator SAmple Consensus (MSAC) algorithm was applied to fit the straight line (polynomial (6)) [35], with maximum distance from the polynomial to an inlier point $d_m = 0.2$ (m). Any points further away are considered outliers (Figure 2). This step provides a table of a and b coefficients for all previously indicated clusters, wherein:

$$y = ax + b \qquad (6)$$

Since rails must be parallel and at an exact distance from each other, they form a track. Therefore, two m and n sections on a line approximated with the polynomial (6) will be parallel if the a coefficients for the P polynomial for the *n*-th cluster (P_n) and the *m*-th cluster P_m are equal, which can be written as:

$$a_n = a_m. \qquad (7)$$

In consequence, two parallel m and n sections lay on a straight line approximated with the polynomial (6) at a distance of D_t, when the *b* coefficients for the P polynomial of the *n*-th (P_n) and *m*-th clusters P_m satisfy the condition:

$$b_m = b_n + D_t\sqrt{1 + a_n^2}, \qquad (8)$$

where: D_t is the standard rail track width, measured between railheads, in metres. Therefore, two polynomials will estimate the parallel course of the rails if they satisfy the condition:

$$P_n \parallel P_m \Rightarrow a_n = a_m \wedge b_m = b_n + D_t\sqrt{1 + a_n^2} \qquad (9)$$

The outcome of filtration based on the expression (9) is a set of polynomial coefficients that are parallel relative to each other and are located at a distance equal to the width of a standard rail track. Therefore, it can be observed that these are only those polynomials that approximate only single point clusters that represent rails. By indicating these points alone, we obtain a fully scrubbed point cloud representing only the rails (Figure 2).
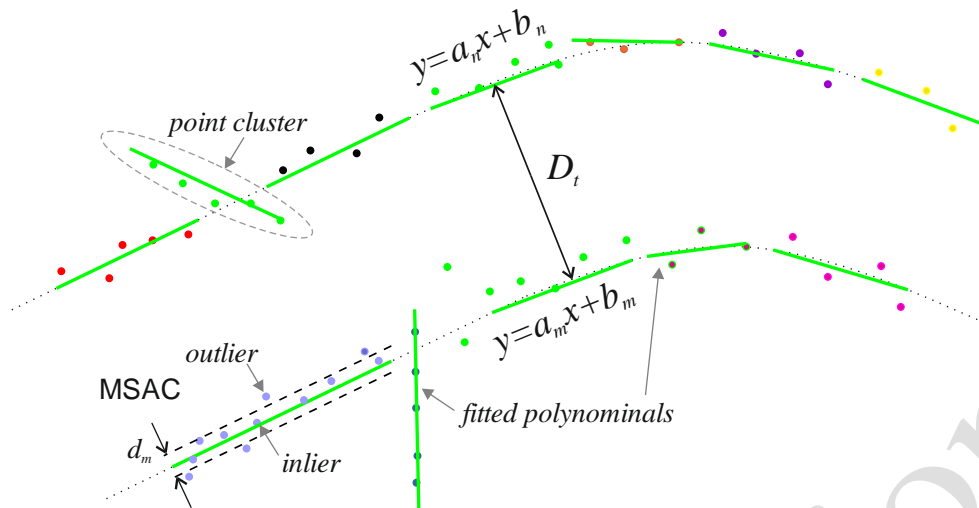
Figure 2. Extraction of points representing rails

3. Results

3.1. *Field data acquisition*

Image data was collected using a typical commercial UAV - UAV DJI Mavic 2 Pro (MP2) (Shenzhen DJI Sciences and Technologies Ltd., China). The study involved conducting a test flight at an altitude of 50 m above ground level (AGL), based on a single grid plan, with a coverage of 70%. The MP2 UAV was equipped with a Hasselbald L1D-20c camera, with a 1'' (13.2x8.8 mm) sensor and a maximum ISO of 12800. This configuration enabled obtaining a ground sampling distance (GSD) equal to 1.16 cm/pix.

Prior to conducting UAV measurements, a photogrammetric matrix consisting of 24 GCP (ground control points) located evenly along the railway line axis was developed. Five of these points were used as study check points (CPs). The positions of all check points were measured with an accurate satellite positioning method - GNSS RTK. GCP position was measured relative to the PL-2000 Polish flat coordinate system, and their altitude was measured relative to the PL-EVRF2007-NH quasigeoid. All checkpoints were marked using special boards.

Photogrammetric models were developed using commercial software Agisoft Metashape ver. 1.6.5 (Agisoft LLC, Russia).

3.2. *Point cloud processing for rail extraction*

The outcomes of the photogrammetric process are typical study products, such as an orthophotomap, digital elevation model and a dense point cloud. The software detected 359 696

tie points, and the dense cloud has 66 512 245 points with a density of 1850 p/m^2. The digital elevation model has a resolution of 2.33 cm/pix, while the orthophotomap has a density of 1.16 cm/pix. The root mean square reprojection error (RMS RE) is 0.683 pix, the total RMSE for control points is 2.85 cm and the total RMSE for check points is 4.95 cm. Basic products have been visualized in Figure 3.
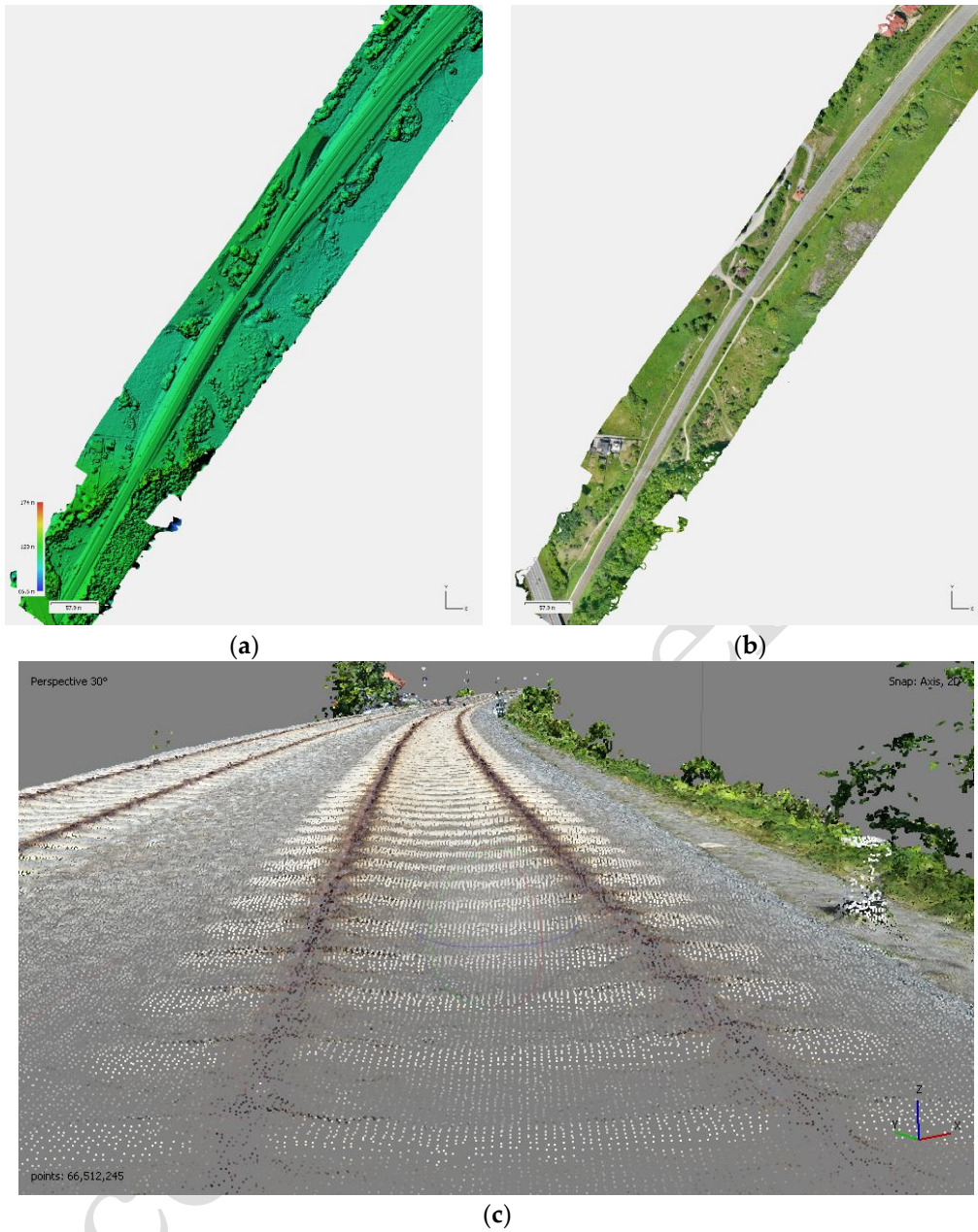
Figure 3. (a) DEM (digital elevation model), (b) orthophotomap, (c) dense point cloud.

In the DEM (digital elevation model), in Figure 3, we can see that (a) the railway embankment clearly has a different elevation than the flat and uniform peak. This embankment is made of bright aggregate, which is visible on the orthophotomap Figure 3 (b). Passing rails can be clearly seen against the background of this aggregate. These two properties enable conducting an initial filtration described in section 2.2. Initial filtration removes elements surrounding the embankment, which exhibit sudden elevation changes and an intensity lower than the pre-set threshold. As can be seen in Figure 3 (c), the UAV point cloud does not enable a clear distinction of track rails, using only the geometric criterion. The rails geometry in z axis (height) is mapped in a softer manner, the change in elevation within them is rather gentle,

which does not enable extracting, as in the case of clouds resulting from laser scanning, where the corresponding rails are very sharp.

Figure 4 shows the results of the initial point cloud filtration. The outcome of this filtration is a pre-cleaned point cloud in which only the points located on a flat surface (3rd eigenvalue <0.001) and with an intensity lower than 200 are visible. The cloud after initial filtration (Figure 4 (c)) includes points (objects) that do not represent rails. This is due to the fact that these conditions are also satisfied by other objects that are to be eliminated at the next filtration stage.
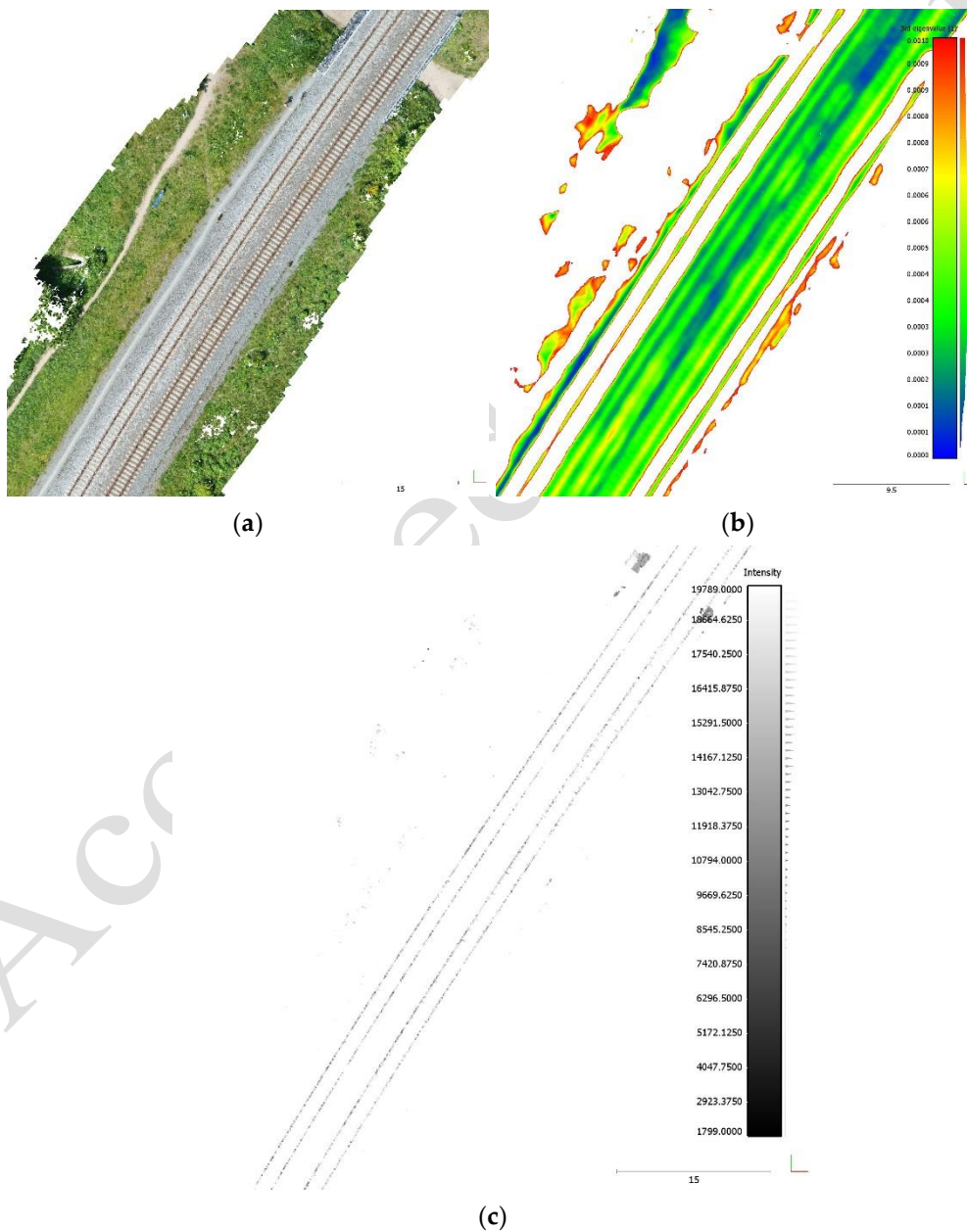

(a)

(b)

(c)

Figure 4. (a) Dense point cloud (selected part), (b) points for 3rd eigenvalue <0.001, (c) points for intensity < 200.

As evident in Figure 4 (b), for the flat part of the railway embankment peak, the 3rd eigenvalues do not rather exceed 0.007 (yellow on the scale), and values about 0.004 are the majority. The 3rd eigenvalue is so sensitive that a rail track course can be seen in some places; however, the value is too small (a maximum of 0.002) to apply only this criterion. Pre-separated flat surfaces within the studied railway track section enable further extraction of pixels with intensities below 200 that probably represent a dark rail - Figure 4(c).

3.3. Track extraction results

After initial filtration, the cloud still has other infrastructural elements that have to be removed. Figure 5(a) shows an example of a cloud fragment with infrastructural residues. In order to enable the reader to precisely compare the results, the figures in the further part of this section will contain the same railway line fragment.

Matching a plane model to a data set using the MSAC method involves its iterative fitting so that the largest possible number falls within the specified threshold (1 meter in this case). This way it is possible, in great approximation, to indicate a certain plane identical to the coplanar course of the rails. Next, by extracting points found at a certain distance from this plane (inliers), it is possible to indicate that belonging to the rails, while eliminating infrastructure located above or below this plane. This operation provides an image representing the rails and adjacent elements, however, without the unnecessary infrastructure (Figure 5(b)).
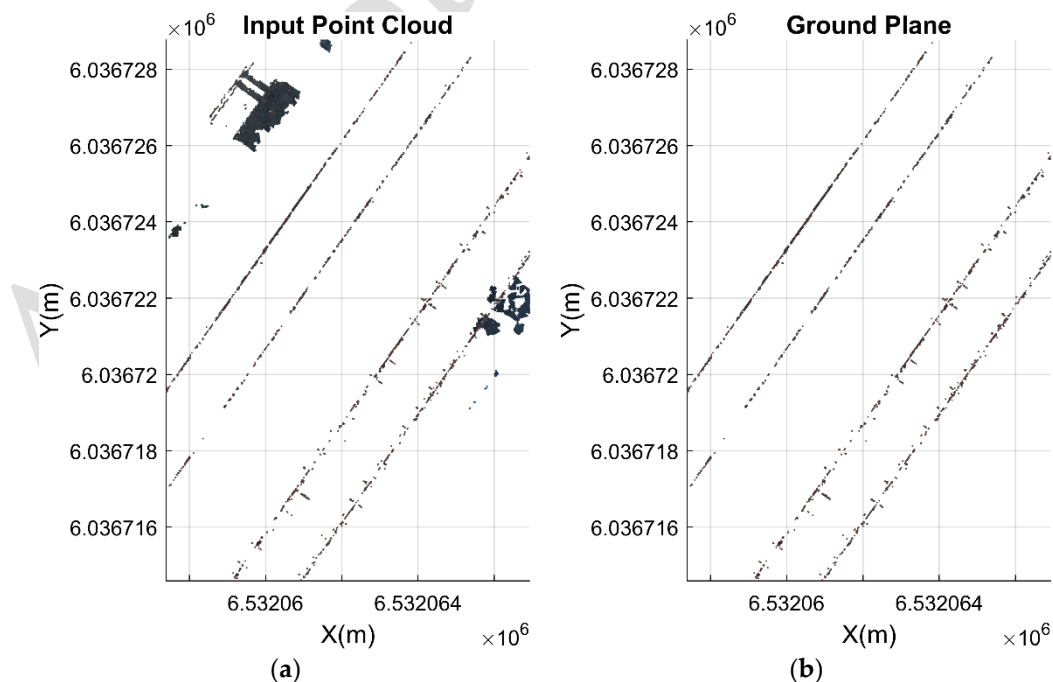

Figure 5. (a) An input railway track fragment, and (b) after eliminating infrastructure with the MSAC method

Extracting coplanar elements eliminates objects standing out from the plane model (b) (outliers). In other words, the geometric extraction covers elements that lie within a common plane with a certain specified tolerance.

Eliminating points with an intensity lower than 200 during initial filtration does not remove and fully clean a cloud, and leaves certain points that represent other objects. They mainly include fasteners and bolts located very near the rail and directly connected with the railway sleepers. Points representing these objects form a kind of a ladder image and are arranged perpendicular to the rail (Figure 5(b). Moreover, the points that represent the rail do not have an equal density, which enables conducting Euclidean segmentation, followed by matching a linear polynomial to such segments. Based on a simplification that a rail runs straight over its certain section, fitting a straight line with a certain minor tolerance will model a rail course within this section.

Figure 6(a) uses different colours to show points belonging to clusters. If the mutual Euclidean distance between points falls within a specified range, these points belong to the same cluster or a certain group of clusters. This group is matched with a linear polynomial using the MSAC method that enables modelling the course of the rails. As can be seen, the small point groups forming the ladder are ignored when matching with the MSAC method, which directly stems from the properties of this method and the set parameters.

Having a complete list of polynomial coefficients for an entire studied point cloud, only that which are parallel and located at a certain distance equal to a railway track width should be indicated. This leads to highlighting only those polynomials that represent rails. By successively indicating the points that are located at a certain distance from the estimating polynomial (points belonging to the rail) and eliminating the non-belonging points, we obtain a point cloud representing only the rails.

The outcome of these operations is a point cloud consisting only of points belonging to the rails, satisfying the aforementioned conditions (Figure 6(b)).
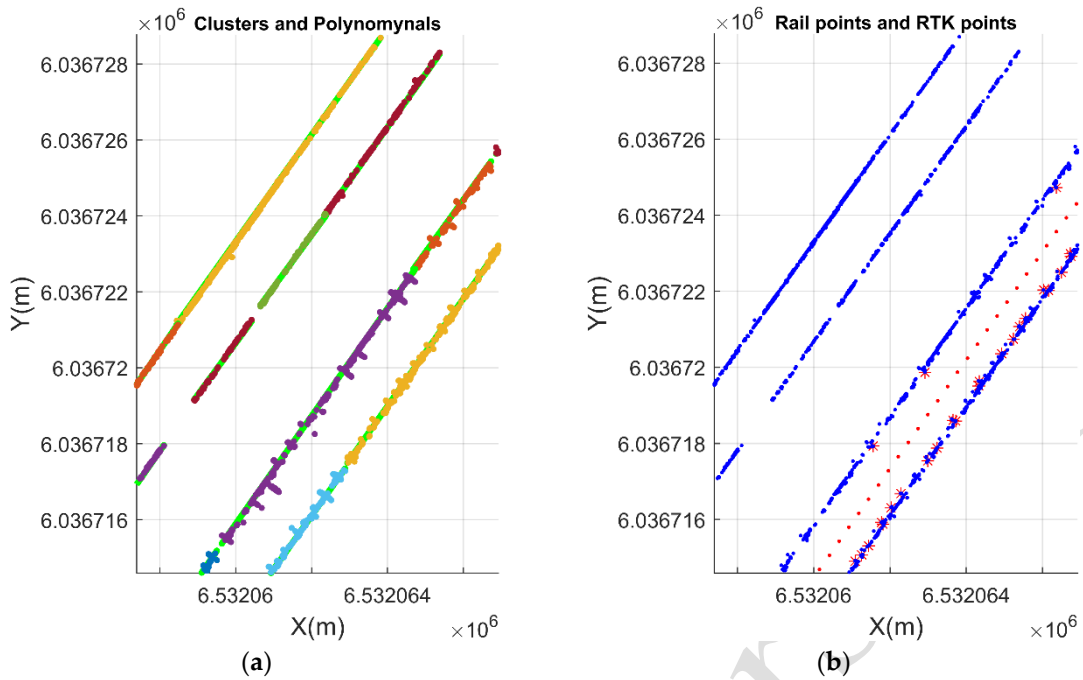
Figure 6. (a) Matched polynomials modelling the rail course (green straights) and points belonging to different clusters (different colours) and (b) indicated points belonging to the rail (blue) and axis points from RTK precise measurement.

3.4 Setting-out of a reference track axis using satellite methods (ground truth)

A ground truth track axis was set out using a special measurement platform (Figure 7) with an installed set of six precise RTK GNSS receivers. The measurement platform was connected to a dedicated locomotive, and such an assembly covered a specified railway line. Dynamic GNSS measurements from all 6 receivers were used to precisely determine the momentary position and orientation of the platform, while the railway track axis positions recorded by receiver E (Figure 7b) were used to determine the reference track axis values, presented within this work. The dynamic GNSS measurement method this area was in fact the only safe method for measuring axis. The researchers did not have the opportunity to make more precise static measurements without stopping rail traffic due to the heavy train traffic on the line.
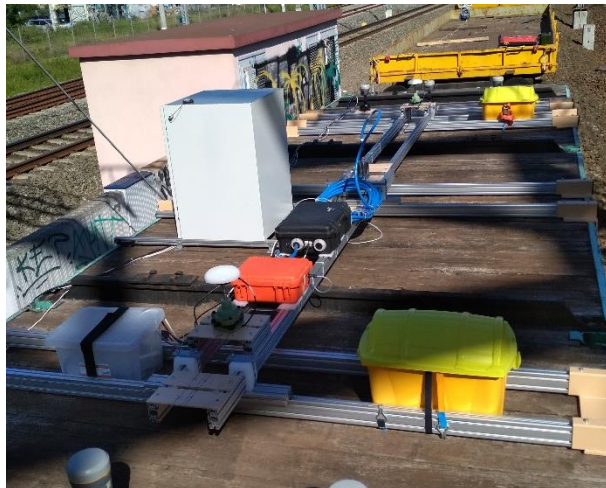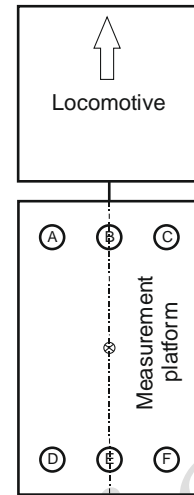
<center>(a)   (b)</center>

Figure 7. (a) Image of a measurement set on a platform, (b) arrangement diagram for RTK GNSS receivers on the platform.

Dynamic satellite measurement accuracies are variable and depend on momentary field barrier conditions and the satellite constellation geometry during the measurements. As a result, one can expect a measurement accuracy within a studied section to vary. Coordinate quality (CQ) coefficient time series in the horizontal plane (2D) and 3D, shown within the studied section, clearly indicates this property (Figure 8). A typical range of 2D and 3D accuracies in this range is 1 to 3 cm. The accuracy for the initial fragment of the measured track decreased to approximately 20 cm. In this section, the line passes near a high forest, where satellite visibility is significantly lower, resulting in a decrease in the dilution of precision (DOP) parameter for satellite measurements.
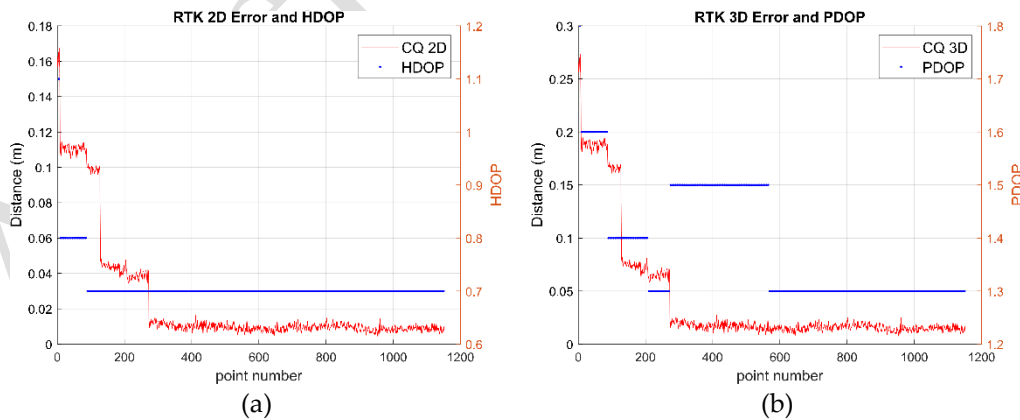
<center>(a)   (b)</center>

Figure 8. (a) Determination accuracy for the track axis reference position within the horizontal plane and the HDOP (horizontal dilution of precision) coefficient, (b) determination accuracy for the track axis reference position within 3D and the PDOP (positional dilution of precision) coefficient.

3.5 Accuracy of presented method

This section presents the accuracies related to setting-out the track axis using the photogrammetric method described herein. The ground truth track axis, to which the photogrammetric measurement will be related, has been set out using a precise dynamic measurement with satellite methods and described in 3.4.

Figure 9 illustrates the deviation of the track axis set out using the photogrammetric method from the reference axis in the horizontal and vertical planes. Figure 10 presents empirical histograms of observed track deviation.
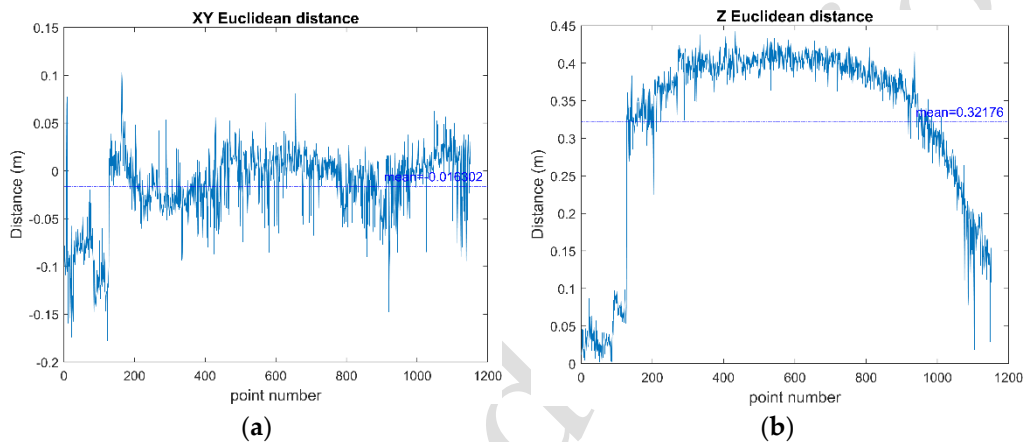

Figure 9. Accuracy of presented method with reference to satellite's measurements (ground truth) in the (a) horizontal and (b) vertical planes.
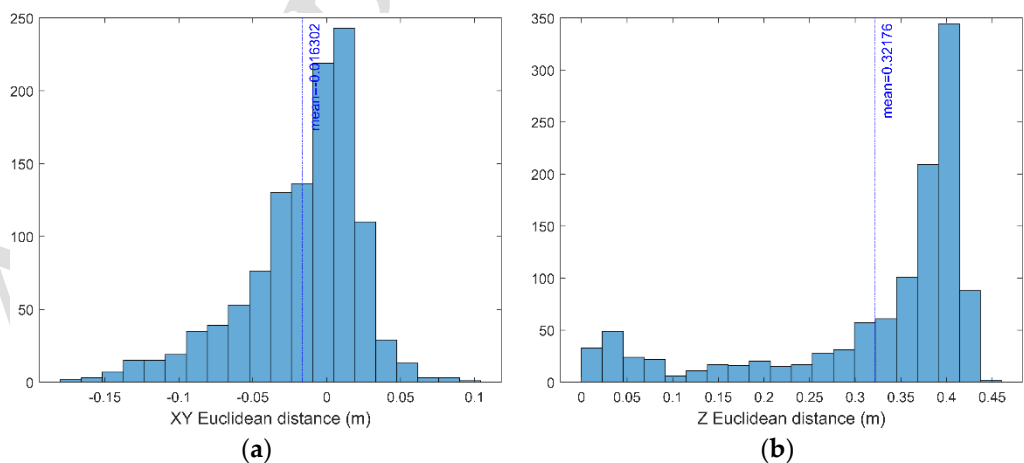

Figure 10. Empirical histograms of track deviation in the (a) horizontal and (b) vertical planes.

The average deviation within the studied section is -0.017 m in the *xy* plane and 0.32 m vertically. The empirical error distribution is presented on Figure 10 in the form of histogram. Analysing the graph of Figure 9 (a) enables the conclusion that measurements are distributed

evenly along the entire studied section. The average axis determination accuracy correlates with GSD and is 1.6 cm. A result like that allows to conclude that the limit of accuracy of the method of extracting the rail line from photogrammetric images is the GSD value. In other words, it can be expected that by increasing the GSD the accuracy will increase, as in the previously presented studies. The initial fragment has a clearly higher deviation from the axis, which varies around -0.1 m. This does not mean that the photogrammetric method in this area exhibits a greater error, but simply confirms the issue of reference position deviation, which exhibits a clearly greater error in this section.

Analysing the graph of Figure 9 (b) reveals that the error in determining the elevation along the studied section clearly increases up to about a half of its length, and then begins to decline. This phenomenon is strictly related to systematic errors appearing at the stage of model development, which is manifested in this case by the appearance of a small topographic doming error. Systematic errors appear at several points within the photogrammetric process and accumulate in the end product. Typical sources of this error include poor image block geometry, internal camera orientation elements and distortion parameters inaccurately determined during calibration, instability of internal camera orientation elements, and inaccurately determined external orientation elements. The accumulation of even small errors in the determination of these parameters over a long section leads to a spherical curve of the surface model, and this curve is proportional to the magnitude of the errors related to these parameters [39]. As demonstrated in [30], erroneous determination of internal orientation elements as a result of autocalibration increases significantly together with declining scene illumination intensity, and has the greatest impact on the correct elevation reconstruction. In the case in question, the topographic doming error within the studied 2 km long section is up to 30 cm. Table 1 shows a statistical summary of achieved results of setting-out the railway track axis using the method discussed herein.

Table 1. Track axis setting-out error using the photogrammetric method - statistical data

	Horizontal plane (x)	Vertical plane (y)
Mean (m)	-0.0168	0.3212
Median (m)	-0.0063	0.3763
Standard deviation (m)	0.0393	0.1211

4. Conclusions

Rail track extraction using geometric features is most often based on point clouds acquired

through mobile laser scanning (MLS). The rails in such scans have a sharp shape, their geometry is clearly visible and they are much higher than the points representing the subgrade. Such a scan enables using methods based on the filtration of point cloud geometric features. In the case of a point cloud created through a photogrammetric process, i.e., aerial photographs taken from a UAV at a certain altitude, rail geometry is not as sharp, as in the case of a mobile laser scan. This hinders a clear indication of relevant features for filtering and separating a studied element. Moreover, such a cloud has well represented object colour mapping, and this enables filtration based on non-geometric features, just like in the case of images. In the case in question, rails are clearly darker than the background, therefore filtration involved eliminating brighter points and leaving only those that corresponded to rail image intensity. Such an approach, combined with pre-cleaning of the cloud and geometric filtration, enabled clearly indicating points representing clouds, and determining track axis course on this basis.

The new method of railroad line extraction based on photogrammetric data presented here is a versatile method and under certain conditions can be applied to extract the track route of any railroad track. Owing to the application of tuned filtration coefficient values, depending on subgrade type and contrast size, it is possible to extract rails placed on various subgrades. This method combines point cloud filtration based on geometric and non-geometric features, making it possible to correctly and precisely extract the rails. The limitations of the method is the contrast between the background and the rail track head being too low, which makes extraction based on spectral response unfeasible. In addition, in the case of a rail dipped in the ground, with no apparent difference in height from the ground, eigenvalue-based filtering will be not possible. UAV-acquired images should be of the best possible quality, as this strongly affects the resulting point cloud and the accuracy of rail line extraction.

A track axis set out using the photogrammetric method has been determined within the studied section with an average accuracy of 1.6 cm in the horizontal plane and 32 cm in the vertical plane. The results correlate with the quality of the source photogrammetric data. By improving the accuracy of the photogrammetric data, it is possible to achieve an even more precise determination of the railroad track axis. The elevation determination error is most impacted by the systematic error (dooming error), which adopted relatively significant values over such a long section.

Please note that track axis measurement with the dynamic GNSS method exhibited significantly lower accuracy on a certain section, reaching even 25 cm in extreme cases. This stems directly from the limited visibility of satellite systems due to high terrain obstacles. The photogrammetric method presented in this article refers to static GNSS measurements applied

for setting-out ground control positions (GCP) used for the image. Such a statistical measurement enables determining GCP position with a greater accuracy, and a photogrammetric image exhibits uniform accuracy throughout its entire horizontal plane space. As a result, as demonstrated in the paper, setting-out a railway track axis will have a constant accuracy within the studied section, equal to the accuracy of a photogrammetric product.

Increasing the upper product accuracy can be achieved by using a high-resolution camera (which enables reducing GSD) and by using a UAV with a GNSS RTK receiver. The dooming error, which cause a rather significant difference in the elevation between extreme and central points of the model, can be relatively simply mitigated by developing additional check points, arranged at the beginning and end of a measurement section. The achieved accuracy enables using data for typical geoinformation, cartographic or stock-taking operation with great reliability.

References

[1]   Singh AK, Swarup A, Agarwal A, et al. Vision based rail track extraction and monitoring through drone imagery. ICT Express. 2019;5:250–255.

[2]   Baltsavias M, Gruen A, van Gool L, et al. Recording, Modeling and Visualization of Cultural Heritage: Proceedings of the International Workshop, Centro Stefano Franscini, Monte Verita, Ascona, Switzerland, May 22-27, 2005. CRC Press; 2005.

[3]   Remondino F. 3D recording for cultural heritage. Remote sensing for archaeological heritage management: proceedings of the 11th EAC Heritage Management Symposium, Reykjavík, Iceland, 25-27 March 2010. 2011.

[4]   Elberink SO, Khoshelham K. Automatic extraction of railroad centerlines from Mobile Laser Scanning data. Remote Sens (Basel). 2015;7:5565–5583.

[5]   Lou Y, Zhang T, Tang J, et al. A Fast Algorithm for Rail Extraction Using Mobile Laser Scanning Data. Remote Sens (Basel). 2018;10:1998.

[6]   Specht M, Stateczny A, Specht C, et al. Concept of an Innovative Autonomous Unmanned System for Bathymetric Monitoring of Shallow Waterbodies (INNOBAT System). Energies (Basel) . 2021;14:5370.

[7]   Oude Elberink S, Khoshelham K, Arastounia M, et al. Rail Track Detection and Modelling in Mobile Laser Scanner Data. ISPRS Annals of the Photogrammetry, Remote Sensing and Spatial Information Sciences . 2013;II-5/W2:223–228.

[8]   Zhu L, Hyyppa J. The Use of Airborne and Mobile Laser Scanning for Modeling Railway Environments in 3D. Remote Sens (Basel) . 2014;6:3075–3100.

[9]   Chen C, Zhang T, Kan Y, et al. A rail extraction algorithm based on the generalized neighborhood height difference from mobile laser scanning data. In: Valenta CR, Shaw JA, Kimata M, editors. SPIE Future Sensing Technologies. SPIE; 2020. p. 18.

[10]   Soni A, Robson S, Gleeson B. Structural monitoring for the rail industry using conventional survey, laser scanning and photogrammetry. Applied Geomatics . 2015;7:123–138.

[11] Beger R, Gedrange C, Hecht R, et al. Data fusion of extremely high resolution aerial imagery and LiDAR data for automated railroad centre line reconstruction. ISPRS Journal of Photogrammetry and Remote Sensing. 2011;66:S40–S51.

[12] Neubert M, Hecht R, Gedrange C, et al. Extraction Of Railroad Objects From Very High Resolution Helicopter-Borne Lidar And Ortho-Image Data. GEOBIA 2008 - Pixels, Objects, Intelligence. Calgary, Alberta, Canada;

[13] Kaleli F, Akgul YS. Vision-based railroad track extraction using dynamic programming. 2009 12th International IEEE Conference on Intelligent Transportation Systems. IEEE; 2009. p. 1–6.

[14] Karakose M, Yaman O, Baygin M, et al. A New Computer Vision Based Method for Rail Track Detection and Fault Diagnosis in Railways. International Journal of Mechanical Engineering and Robotics Research. 2017;6:22–27.

[15] Jiang T, Frøseth GT, Rønnquist A, et al. A robust line-tracking photogrammetry method for uplift measurements of railway catenary systems in noisy backgrounds. Mech Syst Signal Process. 2020;144:106888.

[16] Narazaki Y, Hoskere V, Yoshida K, et al. Synthetic environments for vision-based structural condition assessment of Japanese high-speed railway viaducts. Mech Syst Signal Process. 2021 160:107850.

[17] Singh M, Singh S, Jaiswal J, et al. Autonomous Rail Track Inspection using Vision Based System. 2006 IEEE International Conference on Computational Intelligence for Homeland Security and Personal Safety. IEEE; 2006. p. 56–59.

[18] Karakose M, Yamanand O, Murat K, et al. A New Approach for Condition Monitoring and Detection of Rail Components and Rail Track in Railway*. International Journal of Computational Intelligence Systems. 2018;11:830.

[19] Jarzebowicz L, Judek S. 3D machine vision system for inspection of contact strips in railway vehicle current collectors. 2014 International Conference on Applied Electronics. IEEE; 2014. p. 139–144.

[20] Lei L, Song D, Liu Z, et al. Displacement Identification by Computer Vision for Condition Monitoring of Rail Vehicle Bearings. Sensors. 2021;21:2100.

[21] Liu D, Lu Z, Cao T, et al. A real-time posture monitoring method for rail vehicle bodies based on machine vision. Vehicle System Dynamics. 2017;55:853–874.

[22] Ghassoun Y, Gerke M, Khedar Y, et al. Implementation and Validation of a High Accuracy UAV-Photogrammetry Based Rail Track Inspection System. Remote Sens (Basel). 2021;13:384.

[23] Jarrett C, Perry K, Stol KA. Controller comparisons for autonomous railway following with a fixed-wing UAV. 2015 6th International Conference on Automation, Robotics and Applications (ICARA). IEEE; 2015. p. 104–109.

[24] Guo Y, Li X, Jia L, et al. An Efficient Rail Recognition Scheme Used for Piloting Mini Autonomous UAV in Railway Inspection. 2020 International Conference on Sensing, Diagnostics, Prognostics, and Control (SDPC). IEEE; 2020. p. 284–290.

[25] Banić M, Miltenović A, Pavlović M, et al. INTELLIGENT MACHINE VISION BASED RAILWAY INFRASTRUCTURE INSPECTION AND MONITORING USING UAV. Facta Universitatis, Series: Mechanical Engineering. 2019;17:357.

[26] Sahebdivani S, Arefi H, Maboudi M. Rail Track Detection and Projection-Based 3D Modeling from UAV Point Cloud. Sensors. 2020;20:5220.

[27] Wu Y, Qin Y, Wang Z, et al. A UAV-Based Visual Inspection Method for Rail Surface Defects. Applied Sciences. 2018;8:1028.

[28] Geng Y, Pan F, Jia L, et al. UAV-LiDAR-Based Measuring Framework for Height and Stagger of High-Speed Railway Contact Wire. IEEE Transactions on Intelligent Transportation Systems. 2021;1–14.

[29]   Luo Q, Hu M, Zhao Z, et al. Design and experiments of X-type artificial control targets for a UAV-LiDAR system. Int J Remote Sens. 2020;41:3307–3321.

[30]   Burdziakowski P, Bobkowska K. UAV Photogrammetry under Poor Lighting Conditions—Accuracy Considerations. Sensors. 2021;21:3531.

[31]   Arastounia M. An Enhanced Algorithm for Concurrent Recognition of Rail Tracks and Power Cables from Terrestrial and Airborne LiDAR Point Clouds. Infrastructures (Basel). 2017;2:8.

[32]   Hackel T, Wegner JD, Schindler K. Contour Detection in Unstructured 3D Point Clouds. 2016 IEEE Conference on Computer Vision and Pattern Recognition (CVPR). IEEE; 2016. p. 1610–1618.

[33]   Maalek R, Lichti D, Ruwanpura J. Robust Segmentation of Planar and Linear Features of Terrestrial Laser Scanner Point Clouds Acquired from Construction Sites. Sensors . 2018;18:819.

[34]   Singh AK, Swarup A, Agarwal A, et al. Vision based rail track extraction and monitoring through drone imagery. ICT Express. 2019;

[35]   Torr PHS, Zisserman A. MLESAC: A New Robust Estimator with Application to Estimating Image Geometry. Computer Vision and Image Understanding. 2000;78:138–156.

[36]   Fischler MA, Bolles RC. Random sample consensus. Commun ACM . 1981;24:381–395.

[37]   Rusu RB, Marton ZC, Blodow N, et al. Towards 3D Point cloud based object maps for household environments. Rob Auton Syst. 2008;

[38]   Nguyen A, Le B. 3D point cloud segmentation: A survey. 2013 6th IEEE Conference on Robotics, Automation and Mechatronics (RAM). IEEE; 2013. p. 225–230.

[39]   James MR, Antoniazza G, Robson S, et al. Mitigating systematic error in topographic models for geomorphic change detection: accuracy, precision and considerations beyond off-nadir imagery. Earth Surf Process Landf . 2020;45:2251–2271.